Damped and Driven Breathers and Metastability

Caballero, Daniel A.
Department of Physics
Boston University
dcaba@bu.edu

Wayne, C. Eugene
Department of Mathematics and Statistics
Boston University
cew@math.bu.edu

Abstract

In this article we prove the existence of a new family of periodic solutions for discrete, nonlinear Schrödinger equations subject to spatially localized driving and damping and we show numerically that they provide a more accurate approximation to metastable states in these systems than previous proposals. We also study the stability properties of these solutions and show that they fit well with a previously proposed mechanism for the emergence and persistence of metastable behavior.

1 Introduction and background

In this paper we reexamine the existence and properties of metastable states in (finite) lattices of coupled nonlinear oscillators. Systems of this type have often been used to study energy transport in extended systems and in both stochastic and deterministic versions of these systems it has been observed that the solution can be "trapped" for long times in small regions of the phase space, which in turn affects the length of time it takes for the system to exhibit ergodic properties - in some cases making that time scale so long that these properties are effectively unobservable [1] [2] [3], [4].

In recent work, it has been proven that for chains of oscillators subject to very weak, localized damping, there are open sets of initial data in which this metastable behavior can be approximated for very long times by "breathers", i.e. temporally periodic, spatially localized solutions of the *undamped* equation [5] [6] [7]. The proof used a modulation approach in which the solution of the damped system was decomposed into a breather whose frequency and phase were allowed to vary (slowly) in time, and a correction term which was proven to remain small for very long times.

In the present paper we prove the existence of a new family of breather type solutions which give even better approximations to the metastable states. These are constructed, not by regarding the damped system as a perturbation of the undamped case, but instead by adding an additional *very small* perturbation to the damped system. We prove that this perturbed system has breather solutions, and we show that these new localized states (which we dub *damped and driven breathers*) reproduce aspects of the metastable behavior which the undamped breathers do not. An additional advantage of these solutions is that they allow us to use standard techniques for analyzing the stability of fixed points in studying the metastable states.

We then analyze the stability of these damped and driven breathers (DDB), and conclude with some numerical experiments which both illustrate the effectiveness of the DDB in approximating the metastable state, and also, how this approximation may break down.

1.1 Past results

Following [5] [7], we work with a very specific system of coupled oscillators, namely the discrete nonlinear Schrödinger (dNLS) equation:

$$-i\dot{z}_j = -\epsilon(\Delta z)_j + |z_j|^2 z_j \ , \quad j = 1, 2, \ldots, N \ . \tag{1}$$

Note that if $\epsilon = 0$, this system becomes N, uncoupled, nonlinear oscillators, and we then have trivial, localized, periodic solutions in which one site rotates with non-zero angular frequency, and all other sites have zero amplitude. This is sometimes referred to as the *anti-integrable limit.*

We add a driving term to the first site of our system, and a damping term to the last site by modifying the equation as

$$-i\dot{z}_j = -\epsilon(\Delta z)_j + |z_j|^2 z_j - i\beta\delta_{j,1} z_1 + i\gamma\delta_{j,N} z_N \ , \quad j = 1, 2, \ldots, N \ . \tag{2}$$

The addition of damping and driving to the equation allows one to study energy flow from one end of the system to the other. The existence of breathers in the dNLS equation with localized forcing but distributed damping was studied in [8].

If we now translate to a rotating frame of reference $z_j(t) = e^{i\omega t}\zeta_j$, then

$$-i\dot{\zeta}_j = -\epsilon(\Delta\zeta)_j - \omega\zeta_j + |\zeta_j|^2\zeta_j \ - i\beta\delta_{j,1}\zeta_1 + i\gamma\delta_{j,N}\zeta_N. \tag{3}$$

Finally, we will often want to work with real variables so we decompose $\zeta_j = p_j + iq_j$. Then (3) can be written as the system of differential equations:

$$\dot{p}_j = \epsilon(\Delta q)_j + \omega q_j - (|p_j|^2 + |q_j|^2)q_j + \beta\delta_{j,1}p_1 - \delta_{j,N}p_N \tag{4}$$

$$\dot{q}_j = -\epsilon(\Delta p)_j - \omega p_j + (|p_j|^2 + |q_j|^2)p_j + \beta\delta_{j,1}q_1 - \delta_{j,N}q_N \ . \tag{5}$$

Past research on systems of this type has focused mainly on the Hamiltonian case in which the damping and driving are both absent - i.e. $\gamma = \beta = 0$. In this case,

there is an extensive theory investigating the existence and properties of "breathers". These spatially localized but temporally periodic solutions are known to exist for very general types of lattice of nonlinear Hamiltonian oscillators including the NLS equation, [9] [10] [11].

For the particular case of (4)-(5), one has the following result:

Theorem 1. *(see [7]; Theorem 1.6) If $\beta = \gamma = 0$, there exists $\epsilon_0 > 0$ and $\Delta\Omega > 0$ such that for all $|\epsilon| < \epsilon_0$, and $|\omega - 1| < \Delta\Omega$, the equations (4)-(5) have a family of fixed points $(p_j^*(\epsilon,\omega), 0)$ which vary smoothly with ϵ and ω, and such that $p_1^* = 1 + \mathcal{O}(\epsilon, |1-\omega|)$, $p_j^* = \mathcal{O}(\epsilon^{j-1})$, $j = 2, \ldots, n$, and $q_j^* = 0$.*

Remark 1. *Note that when we say that (4)-(5) has a family of fixed points of the form $(p_j^*(\epsilon,\omega), 0)$, we mean that the q_j components of the fixed point are zero.*

Remark 2. *Due to the invariance of (3) under complex rotations $\zeta_j \to e^{i\theta}\zeta_j$, each of the fixed points constructed in Theorem 1 corresponds to a circle of fixed points.*

Remark 3. *Because the fixed points in Theorem 1 are constructed with the aid of the Implicit Function Theorem, for each (ϵ,ω), they are the unique fixed points in a neighborhood of $p_1 = 1, p_2 = p_3 = \cdots = p_N = 0$ (up to the complex rotation noted in the previous remark).*

Remark 4. *Note that each of the fixed points constructed in Theorem 1 corresponds to a periodic solution with angular frequency ω for (2). If we fix ϵ and consider the family of solutions as a function of ω, combined with the circle of solutions given by the complex rotations we see that in the phase space of (2) we have a cylinder filled with periodic orbits.*

2 Existence and properties of damped and driven breather for NLS

2.1 The implicit function theorem and the existence of breathers for the damped and driven system

Coupled systems of nonlinear oscillators like (2) have often been studied as models for heat transport in solid state matter. In these studies, the first and last oscillator are coupled to stochastic heat baths with different temperatures, to force an energy flow through the system, and a damping term is added to insure that the total energy in the system does not grow without bound. It has been observed that the convergence to the invariant measure in such systems is often extremely slow due to the presence of metastable states in the phase space. In prior work, the energy flow through the system is enforced by placing a localized damping term at one end of the system and placing all the initial energy of the system at the opposite end [12] [5]. One can prove

that the energy in the system tends to zero as $t \to \infty$ and hence it must flow through the system in order to dissipate in this way. In [7] it is proven that for very long times during this dissipative process the system remains in a neighborhood of the cylinder of breather solutions for the undamped system.

In this paper we use the Implicit Function Theorem to construct a new family of solutions for a system subject to both damping and (very weak) driving which we argue provide even better approximations to the metastable states than do the undamped breathers.

Theorem 2. *For ϵ and γ sufficiently small and all ω in a neighborhood of $\omega = 1$, there exists a unique value of β such that the equations (4)-(5) have a stationary solution in a neighborhood of the undamped breather. This family of fixed points depends smoothly on γ, ω and ϵ.*

Remark 5. *Note that stationary solutions of (4)-(5) correspond to periodic solutions with angular frequency ω of (2).*

We begin by defining a function whose components are the equations for $\dot{p}_j$ and $\dot{q}_j$. Thus, we set

$$\begin{aligned} f_j(p_2, p_3, \ldots, p_N, q_2, q_3, \ldots, q_N; \epsilon, \omega, \gamma, p_1, q_1) = \\ = \epsilon(q_{j+1} + q_{j-1} - 2q_j) + \omega q_j - (p_j^2 + q_j^2)q_j \end{aligned} \tag{6}$$

$$\begin{aligned} f_{j+N}(p_2, p_3, \ldots, p_N, q_2, q_3, \ldots, q_N; \epsilon, \omega, \gamma, p_1, q_1) = \\ = -\epsilon(p_{j+1} + p_{j-1} - 2p_j) - \omega p_j + (p_j^2 + q_j^2)p_j \ , \end{aligned} \tag{7}$$

for $j = 2, 3, \ldots N-1$, and

$$\begin{aligned} f_N(p_2, p_3, \ldots, p_N, q_2, q_3, \ldots, q_N; \epsilon, \omega, \gamma, p_1, q_1) = \\ = \epsilon(q_{N-1} - q_N) + \omega q_N - (p_N^2 + q_N^2)q_N - \gamma p_N \end{aligned} \tag{8}$$

$$\begin{aligned} f_{2N}(p_2, p_3, \ldots, p_N, q_2, q_3, \ldots, q_N; \epsilon, \omega, \gamma, p_1, q_1) = \\ = -\epsilon(p_{N-1} - p_N) - \omega p_N + (p_N^2 + q_N^2)p_N - \gamma q_N. \end{aligned} \tag{9}$$

Defining

$$F(p_2, p_3, \ldots, p_N, q_2, q_3, \ldots, q_N; \epsilon, \omega, \gamma, p_1, q_1) = (f_2, f_3, \ldots, f_N, f_{N+2}, f_{N+3}, \ldots, f_{2N}) \ , \tag{10}$$

we see that $F : \mathbb{R}^{2(N-1)} \times \mathbb{R}^5 \to \mathbb{R}^{2(N-1)}$ and that $F(0, 0, \ldots, 0; 0, 1, 0, 1, 0) = 0$. Computing the Jacobian at this fixed point gives:

$$D_{(\tilde{p},\tilde{q})}F = \begin{pmatrix} 0 & 1 \\ -1 & 0 \end{pmatrix} \tag{11}$$

where $\tilde{p} = (p_2, \ldots, p_N)$, $\tilde{q} = (q_2, \ldots, q_N)$, and where 0 represents and $(N-1) \times (N-1)$ matrix of zeros and 1 represents an $(N-1) \times (N-1)$ dimensional identity matrix.

Thus, by the Implicit Function Theorem, for every ϵ, γ, q_1 sufficiently close to zero and every ω and p_1 sufficiently close to 1, there exists (a unique) $p_2^*, \ldots, p_N^*, q_2^*, \ldots, q_N^*$ such that

$$F(p_2^*, p_3^*, \ldots, p_N^*, q_2^*, q_3^*, \ldots, q_N^*; \epsilon, \omega, \gamma, p_1, q_1) = 0 \ . \tag{12}$$

Furthermore, the solution $(p_2^*, \ldots, p_N^*, q_2^*, \ldots, q_N^*)$ depends smoothly (in fact, analytically) on $(\epsilon, \omega, \gamma, p_1, q_1)$.

Finally, consider the two equations for $\dot{p}_1$ and $\dot{q}_1$. In order to have a fixed point, we need

$$f_1(\epsilon, \omega, \beta, p_1, q_1, p_2, q_2) = \epsilon(q_2 - q_1) + \omega q_1 - (q_1^2 + p_1^2)q_1 + \beta p_1 = 0 \tag{13}$$

$$f_{N+1}(\epsilon, \omega, \beta, p_1, q_1, p_2, q_2) = -\epsilon(p_2 - p_1) - \omega p_1 + (q_1^2 + p_1^2)p_1 + \beta q_1 = 0 \tag{14}$$

By rotational invariance, we choose $q_1 = 0$. Then, inserting the solutions q_2^* and p_2^* from above, from the requirement that $f_1 = 0$, we see that we must have

$$\beta p_1 = -\epsilon q_2^* \ , \tag{15}$$

while the requirement that $f_{N+1} = 0$ implies

$$-\epsilon(p_2^* - p_1) - \omega p_1 + p_1^3 = 0 \ . \tag{16}$$

Using the implicit function theorem, and the fact that p_2^* depends smoothly on p_1, we see that there exists a solution p_1^* of (16), for ω near 1 and γ and ϵ sufficiently small which satisfies $(p_1^*)^2 = \omega + \mathcal{O}(\epsilon)$. Inserting this into (15), we see that there is a unique value of β (depending smoothly on ϵ, γ, and ω), such that we have a damped and driven breather near the $(1, 0, 0, \ldots, 0)$ breather, for each value of ω near one and ϵ and γ sufficiently small.

2.2 Approximating the damped and driven breathers

We wish to show that the damped and driven breathers constructed in the previous subsection provide a better approximation to the metastable states that occur during energy dissipation in these systems than do the undamped breathers. To do so, we need accurate approximations to these solutions which we derive in this subsection.

Consider the equations

$$f_j(p_2, p_3, \ldots, p_N, q_2, q_3, \ldots, q_N; \epsilon, \omega, \gamma, p_1, q_1) = 0 \tag{17}$$

$$f_{j+N}(p_2, p_3, \ldots, p_N, q_2, q_3, \ldots, q_N; \epsilon, \omega, \gamma, p_1, q_1) = 0 \ , \tag{18}$$

for $j = 2, \ldots, N$. We want to approximate the solutions of these equations when ϵ and γ are small and p_1 and ω are near 1.

Note the equations for $f_2, \ldots f_{N-1}, f_{N+2}, \ldots, f_{2N-1}$ are the same as those for the undamped breathers, and hence we can construct power-series approximations for

these equations exactly as in the undamped case - i.e., $p_2^* = -\frac{\epsilon p_1}{\omega} + \ldots$, $p_3^* = \frac{\epsilon p_2^*}{\omega} = (\frac{\epsilon}{\omega})^2 p_1 + \ldots, \ldots, p_{N-1}^* = (-\frac{\epsilon}{\omega})^{N-2} p_1 + \ldots$, while all of the q_j^* are zero to this order in ϵ. (See Section 2 of [5] for more details.) Note that because the implicit function theorem guarantees that the solution is analytic and unique, if we can find a consistent power series approximation to the solution to a given order in ϵ, γ, ..., then it must correspond to the actual solution. In order to find the leading order terms in p_N^* and q_N^*, we must look simultaneously at the equations for f_N and f_{2N}. We find that (to lowest order in ϵ and γ) they satisfy:

$$\begin{aligned} \omega q_N^* - \gamma p_N^* &= 0 \\ \epsilon p_{N-1}^* - \omega p_N^* - \gamma q_N^* &= 0 \ . \end{aligned} \tag{19}$$

Inserting our leading order expansion for p_{N-1}^*, and inverting the matrix $\begin{pmatrix} \omega & -\gamma \\ -\gamma & -\omega \end{pmatrix}$, we find:

$$\begin{pmatrix} q_N^* \\ p_N^* \end{pmatrix} = \frac{1}{\omega^2+\gamma^2} \begin{pmatrix} \omega & -\gamma \\ -\gamma & -\omega \end{pmatrix} \begin{pmatrix} 0 \\ \frac{(-1)^{N-2}\epsilon^{N-1}}{\omega^{N-2}} p_1 \end{pmatrix} + \cdots = \begin{pmatrix} \frac{\gamma(-\epsilon)^{N-1} p_1}{\omega^N} \\ (-\frac{\epsilon}{\omega})^{N-1} p_1 \end{pmatrix} + \ldots \tag{20}$$

Using this result for q_N^*, we construct the leading order terms for q_j^* for $j = N-1, N-2, \ldots, 2$. For instance, consider the equation

$$0 = f_{N-1} = \epsilon(q_{N-2}^* + q_N^* - 2q_{N-1}^*) + \omega q_{N-1}^* + ((p_{N-1}^*)^2 + (q_{N-1}^*)^2) q_{N-1}^* \tag{21}$$

Inserting the leading order expression for q_N^* from (20), we find

$$(-1)^{N-1}\gamma \left(\frac{\epsilon}{\omega}\right)^N p_1 + (\omega - 2\epsilon) q_{N-1}^* + \mathcal{O}(\epsilon^{N+1}) = 0 \ , \tag{22}$$

or

$$q_{N-1}^* = (-1)^N \frac{\gamma}{\omega} \left(\frac{\epsilon}{\omega}\right)^N p_1 + \mathcal{O}(\epsilon^{N+1}) \ . \tag{23}$$

Continuing in this way, we find the leading order expression

$$q_j^* = (-1)^{2N-j-1} \frac{\gamma}{\omega} \left(\frac{\epsilon}{\omega}\right)^{2N-j-1} p_1 + \ldots \tag{24}$$

for $j = 2, \ldots, N-1$.

If we now substitute the leading order expression for q_2^* into (15) we calculate that the unique value of β up to leading order is:

$$\beta = (-1)^{2N-2}\gamma \left(\frac{\epsilon}{\omega}\right)^{2N-2} + \cdots = \gamma \left(\frac{\epsilon}{\omega}\right)^{2N-2} + \ldots \tag{25}$$

Remark 6. *The last equality used the fact that $2N-2$ is always even and it shows that the value of β is positive for any choice of N, and also extremely small when N becomes large. The positivity of β is important and natural, since in order to have a steady state in the damped system we expect to need to inject energy at some point, which corresponds to a positive value of β.*

2.3 The "twist" of the breathers

For the undamped breathers, the fixed points all have $q_j^* = 0$ which means that the z_j all lie on the real line within the complex plane - although by rotational invariance, they can be rotated to any line through the origin. In contrast, the damped and driven breathers calculated in the previous section have $q_j^* \neq 0$ for $j > 1$, when $q_1 = 0$. Therefore, the damped and driven breathers do not lie on the same line through the origin. This is the twist of the breathers which we will explore in this section.

An appropriate form of analyzing the twist is by studying the norm and the complex phase of the equations $z_j(t) = r_j(t)e^{i\varphi_j(t)}$. The utility of such a representation in the study of periodic solution of the undamped dNLS equation was noted at least as long ago as [13]. Since we are interested in studying the energy of the system, we can look at the energy of each site individually, defined by $E_j(t) = \frac{1}{2}|z_j(t)|^2$. The system can be represented using these energies and the complex phase. Furthermore, due to rotational invariance we can use the differences in the phases rather than the absolute phases to represent the system. The breather solutions correspond to stationary points of this representation. Calling $\psi_j(t) = \varphi_{j+1}(t) - \varphi_j(t)$ for $j = 1, 2, \ldots, N-1$, the system can be written as follows:

$$\dot{E}_j = -2\epsilon\sqrt{E_jE_{j-1}}\sin\psi_{j-1} + 2\epsilon\sqrt{E_{j+1}E_j}\sin\psi_j + 2\beta\delta_{1,j}E_1 - 2\gamma\delta_{N,j}E_N \tag{26}$$

$$\dot{\psi}_1 = 2(E_2 - E_1)\left(1 + \epsilon\frac{\cos\psi_1}{2\sqrt{E_1E_2}}\right) - \epsilon\sqrt{\frac{E_3}{E_2}}\cos\psi_2 + \epsilon \tag{27}$$

$$\dot{\psi}_j = 2(E_{j+1} - E_j)\left(1 + \epsilon\frac{\cos\psi_j}{2\sqrt{E_jE_{j+1}}}\right) - \epsilon\left(\sqrt{\frac{E_{j+2}}{E_{j+1}}}\cos\psi_{j+1} - \sqrt{\frac{E_{j-1}}{E_j}}\cos\psi_{j-1}\right) \tag{28}$$

$$\dot{\psi}_{N-1} = 2(E_N - E_{N-1})\left(1 + \epsilon\frac{\cos\psi_{N-1}}{2\sqrt{E_{N-1}E_N}}\right) + \epsilon\sqrt{\frac{E_{N-2}}{E_{N-1}}}\cos\psi_{N-2} - \epsilon \tag{29}$$

Remark 7. *Note that an additional advantage of the energy-phase representation is that it uses the rotational invariance of the system to reduce the dimension of the system of equations from $2N$ to $2N-1$.*

Remark 8. *In (26), we set the first term equal to zero if $j = 1$, and the second term equal to zero if $j = N$.*

There is a small change for the two-site system in which case the equations are:

$$\begin{aligned}\dot{E}_1 &= 2\epsilon\sqrt{E_1E_2}\sin\psi + 2\beta E_1 \\ \dot{E}_2 &= -2\epsilon\sqrt{E_1E_2}\sin\psi - 2\gamma E_2 \\ \dot{\psi} &= 2(E_2 - E_1)\left(1 + \epsilon\frac{\cos\psi}{2\sqrt{E_1E_2}}\right)\end{aligned} \tag{30}$$

Because of the simplicity of the two-site system of equations, we can explicitly find all possible damped and driven breathers.

Theorem 3. *For the two-site system with fixed $\beta > 0, \gamma > 0$ such that $\gamma\beta < \epsilon^2$, there exist two families of non-trivial breather solutions (E_1^*, E_2^*, ψ^*) given by:*

(a) If $\beta = \gamma$, we have breathers with $E_1^* = E_2^*$, and $\sin(\psi^*) = -\frac{\beta}{\epsilon}$.

(b) If $E_1^* \neq E_2^*$, then

$$E_1^* = \frac{1}{2}\sqrt{\frac{\gamma}{\beta}}\sqrt{\epsilon^2 - \gamma\beta} \quad E_2^* = \frac{1}{2}\sqrt{\frac{\beta}{\gamma}}\sqrt{\epsilon^2 - \gamma\beta}. \tag{31}$$

If $\epsilon > 0$, we have $\psi^* = -\pi + \arcsin\left(\frac{\sqrt{\gamma\beta}}{\epsilon}\right)$, while if $\epsilon < 0$, we have $\psi^* = -\arcsin\left(\frac{\sqrt{\gamma\beta}}{\epsilon}\right)$.

Note that in (30), if $E_1 = E_2$, $\dot{\psi} = 0$. Adding the first two equations in (30) together implies $2\beta E_1 - 2\gamma E_2 = 0$ at a fixed point, and so, if $E_1 = E_2$, then $\beta = \gamma$. Finally, if $E_1 = E_2$ and $\beta = \gamma$ we see that the RHS of all three equations in (30) are zero if $\sin(\psi^*) = -\frac{\beta}{\epsilon}$. This gives our first family of breathers.

More generally, taking (30) and setting the left hand side to 0, we want the solutions with $E_1 > 0, E_2 > 0, \beta > 0, \gamma > 0, \epsilon \neq 0$. From the first and second equations, we will get:

$$\sin\psi = -\frac{\beta}{\epsilon}\sqrt{\frac{E_1}{E_2}} = -\frac{\gamma}{\epsilon}\sqrt{\frac{E_2}{E_1}}$$

Which leads to $\frac{E_1}{E_2} = \frac{\gamma}{\beta}$. Using this result in the first two equations in (30) implies $\sin\psi^* = -\frac{\sqrt{\gamma\beta}}{\epsilon}$. If $E_1 \neq E_2$, the last equation requires $\cos\psi^* = -\frac{2\sqrt{E_1^* E_2^*}}{\epsilon}$. If $\epsilon > 0$, the fact that the sine of ψ^* is negative and the cosine negative implies that we are in the third quadrant, while if $\epsilon < 0$, we see that ψ^* is in the first quadrant. If we now write $\frac{4E_1E_2}{\epsilon^2} = \cos^2\psi^* = 1 - \sin^2\psi^* = \frac{\beta\gamma}{\epsilon^2}$ and solve for E_1^* and E_2^*, we obtain (31).

Remark 9. *Note that if we take $\beta = \gamma\epsilon^2$, then as $\gamma \to 0$, the solution in (31) converges to the undamped breather near $E_1 = (1/2)$, $E_2 = 0$ and $\psi = 0$ or π, depending on the sign of ϵ.*

This energy-phase representation of the breathers is especially useful when we wish to compare the metastable states which emerge when the damped system is allowed to decay with our breather solutions. In particular, in the undamped, n-site case all the breathers have $\sin\psi_j = 0$ for all j. This means, for example, that if we use the rotational invariance to set $q_1^* = 0$, then all the q_j^* will be equal to zero. However, for nonzero β, γ the equations will lead to $\sin\psi_j \neq 0$.

For the particular breather calculated in Section 2.2, the phase is calculated from $\varphi_j = \arctan(\frac{q_j^*}{p_j^*}) = \frac{q_j^*}{p_j^*} + \dots$. The phases for this breather will be:

$$\varphi_j = \frac{\gamma}{\omega}\left(-\frac{\epsilon}{\omega}\right)^{2(N-j)} + \cdots = \frac{\gamma}{\omega}\left(\frac{\epsilon}{\omega}\right)^{2(N-j)} + \dots \tag{32}$$

With the exception of $\varphi_1 = 0$ as a consequence of choosing $q_1 = 0$. Using this, we find that $\psi_j = \varphi_{j+1} - \varphi_j$ to leading order is simply:

$$\psi_j = \frac{\gamma}{\omega}\left(\frac{\epsilon}{\omega}\right)^{2(N-j-1)} + \dots \tag{33}$$

In particular, we obtain the interesting following result for the last phase difference:

Theorem 4. *For a fixed $\gamma > 0, \omega > 0$, the phase difference between the last two oscillators, ψ_{N-1}, is up to leading order independent of the number of sites. The expression for this phase is:*

$$\psi_{N-1} = \frac{\gamma}{\omega} + \dots \tag{34}$$

Remark 10. *As we will see in the numerical experiments in Section 4, the metastable states we observe during the energy decay in these systems, also exhibit a non-zero "twist" of this type, whose value is very close to that predicted by (34).*

3 Stability

In this section, we examine the stability of the damped and driven breathers constructed above, using the fact that they are fixed points of the equations (4)-(5). Define

$$\tilde{F}(p_1, \dots, p_N, q_1, \dots, q_N, \beta; \epsilon, \omega, \gamma) = (f_1, f_2, \dots, f_N, f_{N+1}, \dots f_{2N}) \ , \tag{35}$$

where the component functions f_j are defined in (6)-(8)-(13).

If we linearize $\tilde{F}$ at the the fixed points $(p^*, q^*) = (p_1^*, \dots, p_N^*, q_1^*, \dots, q_N^*)$, the Jacobian matrix takes the form

$$D_{(p,q)}\tilde{F}\big|_{(p^*,q^*)} = \begin{pmatrix} D^{(1)} & A^{(\omega,\epsilon)} \\ B^{(\omega,\epsilon)} & D^{(2)} \end{pmatrix} \tag{36}$$

Here, $A^{(\omega,\epsilon)}$ and $B^{(\omega,\epsilon)}$ are $N \times N$ tri-diagonal matrices and $D^{(1)}$ and $D^{(2)}$ are $N \times N$ diagonal matrices. More precisely, the matrix $A^{(\omega,\epsilon)}$ has ϵ on the sub- and super-diagonal, while the diagonal elements are $\omega - a_j\epsilon - (p_j^*)^2 - 3(q_j^*)^3$, $j = 1, 2, \dots, N$, where $a_1 = 1$, $a_N = 1$ and all other $a_j = 2$. The matrix $B^{(\omega,\epsilon)}$ has sub- and super-diagonal elements equal to $-\epsilon$, while the diagonal elements are $-\omega + a_j\epsilon + 3(p_j^*)^2 + (q_1^*)^2$. The diagonal matrix $D^{(1)}$ has diagonal elements $D^{(1)}_{jj} = \beta\delta_{1,j} - \gamma\delta_{N,j} - 2p_j^*q_j^*$, while $D^{(2)}$ has matrix elements $D^{(2)}_{jj} = \beta\delta_{1,j} - \gamma\delta_{N,j} + 2p_j^*q_j^*$. Note that from the approximations to p_j^* and q_j^* derived in Subsection 2.2, we see that $D^{(k)}_{jj} = -\gamma\delta_{j,N} + \mathcal{O}(\gamma\epsilon^{2(N-1)})$. Thus, the diagonal part of the Jacobian is dominated by the dissipation coming from γ.

To make the form of the Jacobian matrix more explicit, we write out the form of the submatrices for $N = 3$. We have

$$A^{(\omega,\epsilon)} = \begin{pmatrix} \omega - \epsilon - (p_1^*)^2 - 3(q_1^*)^2 & \epsilon & 0 \\ \epsilon & \omega - 2\epsilon - (p_2^*)^2 - 3(q_2^*)^2 & \epsilon \\ 0 & \epsilon & \omega - \epsilon - (p_3^*)^2 - 3(q_3^*)^2 \end{pmatrix}, \tag{37}$$

$$B^{(\omega,\epsilon)} = \begin{pmatrix} -\omega + \epsilon + 3(p_1^*)^2 + (q_1^*)^2 & -\epsilon & 0 \\ -\epsilon & -\omega + 2\epsilon + 3(p_2^*)^2 + (q_2^*)^2 & -\epsilon \\ 0 & -\epsilon & -\omega + \epsilon + 3(p_3^*)^2 + (q_3^*)^2 \end{pmatrix}, \tag{38}$$

$$D^{(1)} = \begin{pmatrix} \beta^* - 2p_1^*q_1^* & 0 & 0 \\ 0 & -2p_2^*q_2^* & 0 \\ 0 & 0 & -\gamma - 2p_3^*q_3^* \end{pmatrix}, \tag{39}$$

and finally,

$$D^{(2)} = \begin{pmatrix} \beta^* + 2p_1^*q_1^* & 0 & 0 \\ 0 & 2p_2^*q_2^* & 0 \\ 0 & 0 & -\gamma + 2p_3^*q_3^* \end{pmatrix}. \tag{40}$$

Note that because of the γ dependence of q_j^* and β^*, both $D^{(1)}$ and $D^{(2)}$ vanish in the $\gamma = 0$ limit, as do all the terms involving (q_j^*) in the matrices $A^{(\omega,\epsilon)}$ and $B^{(\omega,\epsilon)}$. Thus the Jacobian reduces to the Jacobian of the linearization of the undamped breather. The spectrum of this matrix when $\epsilon > 0$ was analyzed in detail in prior work [7]. The same methods used in Theorem 5.1 of that reference also apply to the case when $\epsilon < 0$ and we find that if $\gamma = 0$, the matrix $D_{(p,q)}\tilde{F}\big|_{(p^*,q^*)}$ has:

- a two-dimensional zero eigenspace, spanned by the derivatives of the family of breathers with respect to the frequency and phase of the breather, and
- $(N-1)$ simple, purely imaginary eigenvalues near $+i$, separated by a distance $\sim C\epsilon$ from each other, and
- $(N-1)$ simple, purely imaginary eigenvalues near $-i$ that are similarly separated.

The next thing we note is that by the results of Section 2.2, the elements β^*, and $2p_j^*q_j^*$ in $D^{(1)}$ and $D^{(2)}$ are much smaller than γ (smaller by a factor of $\mathcal{O}(\epsilon^{2(N-1)})$.) The effects of perturbing the simple eigenvalues of the undamped Jacobian matrices by the simplified, lower order diagonal matrices

$$\bar{D}_{ij}^{(k)} = \begin{cases} -\gamma & \text{if } \ i = j = N \\ 0 & \text{otherwise .} \end{cases}$$

where $k = 1, 2$ and $1 \le i, j \le N$ was considered in [7] and by using those methods, one can show that the $2(N-1)$ simple, imaginary eigenvalues near $\pm i$ all perturb to

simple eigenvalues with negative real parts satisfying

$$\mathrm{Re}(\lambda_j) \leq -C(N)\gamma \ , \tag{41}$$

where $C(N)$ is a constant depending on N, but independent of γ or ϵ.[1]

If we now consider the effects of including the elements β^* and $2p_j^*q_j^*$ in $D^{(1)}$ and $D^{(2)}$ and the additional diagonal elements proportional to $q(j^*)^2$ in $A^{(\omega,\epsilon)}$ and $B^{(\omega,\epsilon)}$, then again from the results of the perturbation theory of simple eigenvalues, [14], the shift in these eigenvalues is proportional to $\gamma\epsilon^{2(N-1)}$. In particular, for ϵ sufficiently small, these eigenvalues remain simple and still satisfy the bound (41), though possibly with a slightly smaller value of $C(N)$.

We next note that the Jacobian matrix for the linearization at the damped and driven breather has a zero eigenvalue with explicitly computable eigenvector. This is due to the invariance of (3) under complex rotations $\zeta \to e^{i\phi}\zeta$. If we write the equations (35) in terms of $\zeta_j = p_j + iq_j$, (and in a slight abuse of notation still denote the function whose zeros give the fixed points by $\tilde{F}$,) we see that

$$\tilde{F}(e^{i\phi}\zeta_1^*, e^{i\phi}\zeta_2^*, \ldots, e^{i\phi}\zeta_N^*, \beta^*; \epsilon, \omega, \gamma) = \tilde{F}(\zeta_1^*, \zeta_2^*, \ldots, \zeta_N^*, \beta^*; \epsilon, \omega, \gamma) = 0 \ , \tag{42}$$

for all ϕ. Thus, if we differentiate with respect to ϕ and then set $\phi = 0$, we find

$$D_\zeta \tilde{F}|_{\zeta^*}(i\zeta^*) = 0 \ , \tag{43}$$

or, returning to our (p, q) coordinates, we see that the Jacobian has a zero eigenvalue, with eigenvector

$$\mathbf{v}^{(0)} = \begin{pmatrix} -q^* \\ p^* \end{pmatrix} \ . \tag{44}$$

One might expect the zero-eigenspace of the Jacobian to be two-dimensional due to the family of fixed points as one varies ω. This turns out not to be the case (as near as we can tell) due to the dependence of the parameter β on ω. More precisely, suppose one differentiates the fixed-point equation

$$F(\zeta_1^*(\omega), \zeta_2^*(\omega), \ldots, \zeta_N^*(\omega), \beta(\omega); \epsilon, \omega, \gamma) = 0 \ , \tag{45}$$

with respect to ω. We find

$$D_{(p,q)}\tilde{F}|_{(p^*,q^*)} \begin{pmatrix} \partial_\omega q^* \\ \partial_\omega p^* \end{pmatrix} + \begin{pmatrix} q^* \\ -p^* \end{pmatrix} + \begin{pmatrix} (\partial_\omega \beta^*) q_1^* \\ 0 \\ (\partial_\omega \beta^*) p_1^* \\ 0 \end{pmatrix} = 0 \ . \tag{46}$$

Here, the final vector in (46) is a $2N$ dimensional vector whose first element is $(\partial_\omega \beta^*)q_1^*$, followed by $(N-1)$ zeros, then the $(\partial_\omega \beta^*)p_1^*$ and another $(N-1)$ zeros. Thus, we see that the Jacobian matrix maps the vector $(\partial_\omega q^*, \partial_\omega p^*)^T$ onto the

[1] The form of the estimate in (41) differs slighly from that found in Theorem 6.1 of the prior work [7] because the parameter called γ in this paper was called $\gamma\epsilon$ in that work.

zero eigenvector, plus the very small correction $((\partial_\omega \beta^*) q_1^*, 0, (\partial_\omega \beta^*) p_1^*, 0)^T$. (Note that this last vector has norm $\mathcal{O}(\epsilon^{2(N-1)})$.)

Thus, we expect that this remaining eigenvalue is non-zero, but very small, a conjecture born out by the numerical experiments of the next subsection.

Summing up, we have shown that the Jacobian matrix of the linearization of the equations of motion at the damped and driven breathers:

- One zero eigenvalue.
- $2(N-1)$ complex eigenvalues with negative real parts satisfying (41).
- One eigenvalue which we conjecture is very small, and which on the basis of our numerics is positive.

3.1 Numerical investigation of stability

The remaining eigenvalue proves challenging to analyze so we first look at the two-site case due to its simplicity. From the result of Theorem 3 we obtain that the Jacobian at the breather is:

$$D_{(p,q)}F = \begin{pmatrix} \beta & 0 & 2E_2^* & \epsilon \\ 0 & -2\beta(1-\frac{\gamma\beta}{\epsilon^2}) - \gamma & \epsilon & -4E_2^*\frac{\gamma\beta}{\epsilon^2} + 2E_1^* \\ 4E_1^* - 2E_2^* & -\epsilon & \beta & 0 \\ -\epsilon & 4E_2^*(1-\frac{\gamma\beta}{\epsilon^2}) - 2E_1^* & 0 & 2\beta(1-\frac{\gamma\beta}{\epsilon^2}) - \gamma \end{pmatrix} \tag{47}$$

Note that in simplifying the form of the Jacobian matrix we have repeatedly used that for the breather constructed in Theorem 3, one has $\omega - \epsilon = 2(E_1^* + E_2^*)$.

We used Mathematica to solve the characteristic polynomial and find the eigenvalues. After inserting the approximate value of β for the two-site case in accordance to (15), the results for the nonzero eigenvalues are:

$$\mu_1 = 4\gamma\left(\frac{\epsilon}{\omega}\right)^2 + \mathcal{O}(\gamma\epsilon^4) \tag{48}$$

$$\mu_2 = -\gamma\left(1 + \left(\frac{\epsilon}{\omega}\right)^2 + \mathcal{O}(\epsilon^4)\right) + i\left(\omega + \mathcal{O}(\epsilon^2)\right) \tag{49}$$

$$\mu_3 = -\gamma\left(1 + \left(\frac{\epsilon}{\omega}\right)^2 + \mathcal{O}(\epsilon^4)\right) - i\left(\omega + \mathcal{O}(\epsilon^2)\right) \tag{50}$$

The eigenvalue we could not compute through other methods turned out to be small and positive. We can also look at the Jacobian for the Energy-phase representation, which at the breather is:

$$\begin{pmatrix} \beta & -\gamma & -(\varepsilon^2-\gamma\beta) \\ \beta & -\gamma & (\varepsilon^2-\gamma\beta) \\ -1+\frac{\beta}{\gamma} & 1-\frac{\gamma}{\beta} & \beta-\gamma \end{pmatrix} \tag{51}$$

Once again we used Mathematica to solve the characteristic polynomial and after inserting the approximate value of β, the eigenvalues are (up to leading order) the same as those in (48), (49), (50).

To better understand the instability caused by this positive eigenvalue we can look at the corresponding eigenvector. In the energy-phase representation, numerical evaluation of the eigenvector leads us to propose that the eigenvector is, up to leading order, expressed as:

$$\mathbf{v}_1 = \begin{pmatrix} 1 \\ -\frac{\epsilon^2}{\omega^2} \\ -2\frac{\gamma}{\omega^2} \end{pmatrix} + \dots \tag{52}$$

The error in this approximation can be estimated from $||D_{E,\psi}\mathbf{v}_1 - \mu_1\mathbf{v_1}||$ which is of order $\mathcal{O}(\frac{\gamma^2}{\omega^2} + \gamma\frac{\epsilon^4}{\omega^4})$.
On the other hand, we can compute a vector pointing in the direction of the family of breathers by differentiating the analytic expression for the breather with respect to ω. The calculation is as follows:

$$\frac{\partial}{\partial\omega}\begin{pmatrix} \frac{1}{2}\omega \\ \frac{1}{2}\frac{\epsilon^2}{\omega} \\ \frac{\gamma}{\omega} \end{pmatrix} + \dots = \frac{1}{2}\begin{pmatrix} 1 \\ -\frac{\epsilon^2}{\omega^2} \\ -2\frac{\gamma}{\omega^2} \end{pmatrix} + \dots \tag{53}$$

Thus, the vector describing the direction of the family of breathers is - up to leading order - in the same direction as the eigenvector corresponding to the positive eigenvalue in (52).

We conjecture that there is always a (very small) positive eigenvalue with an eigenvector approximately pointing roughly in the same direction as the family of breathers. Assuming this spectral picture is correct, initial conditions chosen close to the family of damped and driven breather would be attracted toward the cylinder of fixed points (due to the fact that the eigenvalues corresponding to directions normal to this cylinder all have negative real part) while we have a very slow drift along the cylinder, corresponding to the one positive eigenvalue. Eventually, when either higher order corrections become important, or when the family of breathers disappears through a bifurcation, this approximation will break down. Our numerical experiments in the next section indicate that it is the second of these scenarios which actually leads to the breakdown of the approximation by breathers.

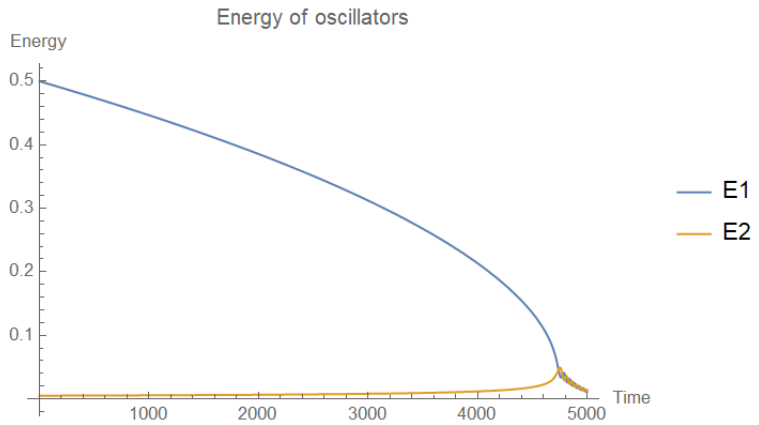

Figure 1: The energy of each oscillator in the two-site system. The parameters chosen were $\omega_0 = 1, \gamma = 0.005, \epsilon = -0.1$ and the initial conditions correspond to the approximation to the damped and driven breathers from Section 2.2.

4 Numerical verification

In this section, we present the results of numerical experiments to illustrate the results of the preceding sections. We focus on systems with a small number of sites (specifically, $N = 2, 3$) because the very slow drift along the family of breathers means that the computational time required increases very rapidly with N. In addition, by concentrating on these small systems we are able to perform many computations explicitly, which helps to elucidate the numerical results. All numerical computations are done with Mathematica using the LSODA method.

We choose as initial conditions for our numerics the approximation to the damped and driven breather computed in Section 2.2. This in turn requires us to choose a value for ω_0, our initial approximation to angular frequency of the breather. We then set $p_1 = \sqrt{\omega_0}$. We can approximate the initial values for the other variables using the equations of motion and our knowledge of the breather solution. For example, when the solution is close to a damped and driven breather we can consider $\dot{\psi}_j \approx 0$ and so all the $\dot{\varphi}_j$ are the same. For this reason, we can define $\omega(t)$ to be any of the $\dot{\varphi}_j$ and we should obtain approximately the same result. For simplicity, we define it as $\omega(t) = \dot{\varphi}_1(t)$ and in turn we can calculate it from:

$$\dot{\varphi}_1 = 2E_1 + \epsilon - \epsilon\sqrt{\frac{E_2}{E_1}}\cos\psi_1 \tag{54}$$

Notice that $\omega_0 \neq \omega(0)$ because of the fact that we calculate an approximation to p_1 from ω_0 and then use it to calculate approximations for $E_1(0), E_2(0), \psi_1(0)$. In fact $\omega_0 = 2E_1(0)$.

We begin by looking at the evolution of the energy-site for the two and three site

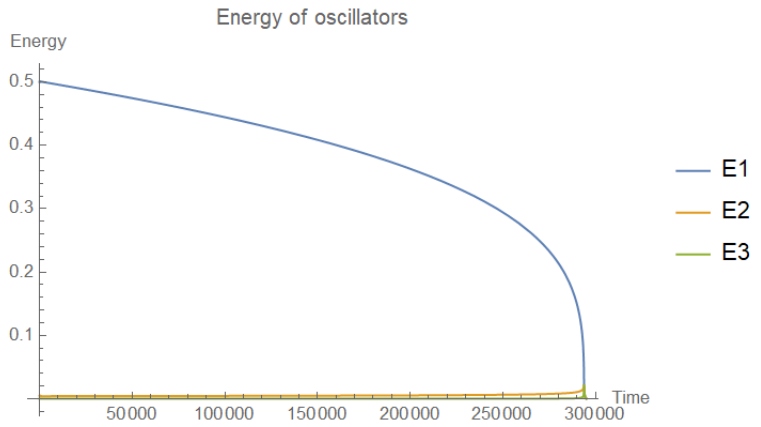

Figure 2: The energy of each oscillator in the three-site system. The parameters chosen were then same as in Figure 1 and the initial conditions correspond to the approximation to the damped and driven breathers from Section 2.2.

systems. These calculations are presented in Figures 1 and 2.

We note that in both cases, the solution remains close to the breather for very long times - much longer for the three-site case than the two-site case, illustrating the fact that these metastable states have a much greater impact on the equilibration of the system as the number of sites grows.

We now show that the damped and driven breathers provide a more accurate approximation to the metastable states than the undamped breathers. Recall that for the undamped breathers in the $(p.q)$ representation, $q_j^* = 0$ (see Theorem 1). Thus, the "twist" angle ψ_j, discussed in section 2.3 is either 0 or π for all j. On the other hand, the damped and driven breathers have non-zero twist whose value is related to γ and ω, and we show that this is also true for the metastable state and that our approximate formula for the twist derived above provides a good approximation to the twist of the metastable states.

The phase difference for the two-site system is graphed in Figure 3. The blue line corresponds to the solution computed by Mathematica. The first important result is that the phase difference is nonzero, as we predicted from the calculations for the damped and driven breathers, proving the existence of the twist. The orange line corresponds to the function $\frac{\gamma}{\omega(t)}$. This function is the instantaneous highest order approximation to the twist of the damped and driven breather derived in Theorem 4. The value of $\omega(t)$ is calculated from (54). Recall that $\omega(t) \approx p_1(t)^2 \approx 2E_1(t)$. We have also included in Figure 3 the green curve, which plots $\frac{\gamma}{2E(t)}$ and which numerically seems to provide a better approximation to the twist. At the moment, we do not have an explanation of why it gives a better approximation though presumably it results from the higher order terms omitted in the approximation of either $\omega(t)$ or ψ_j.

Note that from graph (a) in Figure 3 we see that with either approximation, the

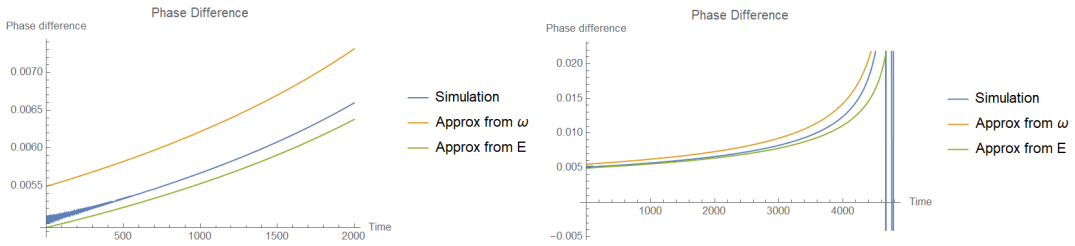

Figure 3: Graph of the phase difference and its approximation for the same parameters and initial conditions as Figure 1; (a) is graphed between times 0 and 2000, and (b) between times 0 and 4800, approximately when it leaves the metastable state.

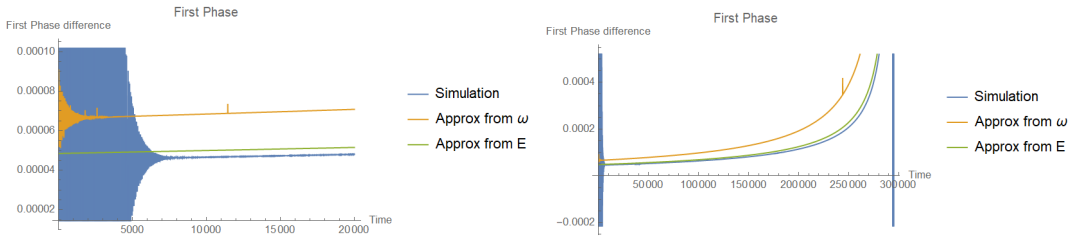

Figure 4: Graph of the phase difference between the first and second oscillator and its approximation for the same parameters and initial conditions as Figure 2; (a) is graphed between times 0 and 20 000, and (b) between times 0 and 295 000, approximately when it leaves the metastable state.

error in the approximation of the twist is less than 10% for a very long period. Graph (b) in this Figure shows that the twist metastable state is well approximated by the twist of the damped and driven breather until shortly before the time ($t \approx 4800$) at which time the breather solution breaks down. This bifurcation is analyzed in more detail in subsection 4.1.

Figure 4 and Figure 5 are the graphs in the three-site system for $\psi_1(t)$ and $\psi_2(t)$ respectively. The blue, orange and green lines have the same meaning as in Figure 3. The same observations that applied for the phase of the two-site system also apply to those of the three-site system. However, the effectiveness of approximating the phase using E seems to have increased while the approximation using ω has become less accurate.

Speaking colloquially, our numerics show that the metastable state slides along the family of damped and driven breathers. This is consistent with our numerical observation that the eigenvector corresponding to the positive eigenvalue of the linearization points along the direction of the family of breathers.

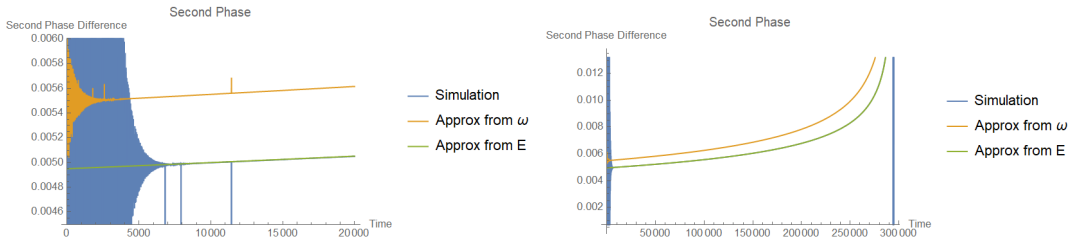

Figure 5: Graph of the phase difference between the second and third oscillator and its approximation for the same parameters and initial conditions as Figure 2; (a) is graphed between times 0 and 20 000, and (b) between times 0 and 295 000, approximately when it leaves the metastable state.

4.1 Detailed analysis of the two-site system

For the two-site system, we do not have to limit the analysis to just the metastable breather we have studied so far, but can make a more global investigation of the phase space. This analysis is better suited to using the energy-phase equations rather than expressing the system in the p, q coordinates.

For the undamped case (i.e. (30) with $\beta = \gamma = 0$), all breather solutions were found in [13] and in our notation they take the form:

$$E_1^{(1)} = \frac{1}{2}E \qquad E_2^{(1)} = \tfrac{1}{2}E \qquad \psi^{(1)} = 0 \tag{55}$$

$$E_1^{(2)} = \frac{1}{2}E \qquad E_2^{(2)} = \tfrac{1}{2}E \qquad \psi^{(2)} = \pi \tag{56}$$

$$E_1^{(3)} = \frac{1}{2}\left(E + \sqrt{E^2 - \epsilon^2}\right) \qquad E_2^{(3)} = \tfrac{1}{2}\left(E - \sqrt{E^2 - \epsilon^2}\right) \qquad \psi^{(3)} = \pi \tag{57}$$

$$E_1^{(4)} = \frac{1}{2}\left(E - \sqrt{E^2 - \epsilon^2}\right) \qquad E_2^{(4)} = \tfrac{1}{2}\left(E + \sqrt{E^2 - \epsilon^2}\right) \qquad \psi^{(4)} = \pi \tag{58}$$

when $\epsilon > 0$ with similar expressions for $\epsilon < 0$.

For each of these breathers, we can calculate the angular frequency ω from E. The values are $\omega^{(1)} = E, \omega^{(2)} = E + 2\epsilon, \omega^{(3)} = \omega^{(4)} = 2E + \epsilon$. The third breather is the one close to the metastable states discussed so far.

For $|\epsilon| >> \gamma > 0$ but $\beta = 0$, the breathers disappear but they can be used to help find solutions of the damped problem. For example, if we make the *Ansatz* that $E_1(t) = E_2(t)$ for all time, and substitute this into the equations of motion we find exact solutions:

$$E_1(t) = \tfrac{1}{2}E_0 e^{-\gamma t} \qquad E_2(t) = \tfrac{1}{2}E_0 e^{-\gamma t} \qquad \psi(t) = -\arcsin\left(\frac{\gamma}{2\epsilon}\right) \tag{59}$$

$$E_1(t) = \tfrac{1}{2}E_0 e^{-\gamma t} \qquad E_2(t) = \tfrac{1}{2}E_0 e^{-\gamma t} \qquad \psi(t) = -\pi + \arcsin\left(\frac{\gamma}{2\epsilon}\right) \tag{60}$$

where $E_0 = E_1(0) + E_2(0)$ is the initial total energy, and $\epsilon > 0$. One has similar expressions when $\epsilon < 0$.

We can use a similar argument to approximate the effects of initial conditions close to the solution $E^{(3)}$ of (55). First, differentiate $\frac{d}{dt}E_1^{(3)}$ and $\frac{d}{dt}E_2^{(3)}$:

$$\frac{d}{dt}E_1^{(3)} = \frac{1}{2}\dot{E}\left(1 + \frac{E}{\sqrt{E^2-\epsilon^2}}\right) \quad \frac{d}{dt}E_2^{(3)} = \frac{1}{2}\dot{E}\left(1 - \frac{E}{\sqrt{E^2-\epsilon^2}}\right)$$

Using $\dot{E} = \dot{E}_1 + \dot{E}_2 = -2\gamma E_2$, and considering $E_1 = E_1^{(3)}, E_2 = E_2^{(3)}$, we set $\frac{d}{dt}E_1^{(3)} - \frac{d}{dt}E_2^{(3)} = \dot{E}_1 - \dot{E}_2$ and solve for $\sin\psi$. The result will be:

$$\sin\psi = \frac{\gamma}{2\sqrt{E^2-\epsilon^2}} \tag{61}$$

Note that this is only an approximation to the solution - this value of ψ will not satisfy the equation for $\dot{\psi}$. However Figure 6 shows that it is a very accurate approximation when $E \gtrsim |\epsilon|$. Recall that for this breather $\omega^{(3)} = 2E + \epsilon$, so calculating the leading order in ψ we find $\psi = \frac{\gamma}{\omega} + \ldots$, which is identical to the value of the twist in the damped and driven breather from Theorem 4. This is further evidence of the fact that the damped and driven breathers provide a better approximation to the metastable states than do the undamped breathers.

We also obtain an approximation to the time evolution of the energy through:

$$\dot{E} = -2\gamma E_2 \approx -2\gamma E_2^{(3)} = -\gamma\left(E - \sqrt{E^2-\epsilon^2}\right) \tag{62}$$

If the system starts with initial total energy E_0, an approximate expression for $E(t)$ can be calculated by solving the differential equation to obtain:

$$E(t) \approx \frac{|\epsilon|}{2}\left(\sqrt{-W_{-1}\left(-e^{-1+4\gamma(t-\tau)}\right)} + \frac{1}{\sqrt{-W_{-1}\left(-e^{-1+4\gamma(t-\tau)}\right)}}\right) \tag{63}$$

Here W_{-1} is the -1 branch of the product logarithm, and τ is the time for which $\lim_{t\to\tau} E(t) = |\epsilon|$ and is given by:

$$\tau = \frac{1}{2\gamma}\left(E_0\frac{E_0 + \sqrt{E_0^2-\epsilon^2}}{\epsilon^2} - \ln\left(\frac{E_0 + \sqrt{E_0^2-\epsilon^2}}{|\epsilon|}\right) - 1\right) \tag{64}$$

If the solution found was exact, τ would be the time when $E = |\epsilon|$, corresponding to the bifurcation for the undamped system, therefore the solution would be valid up until τ. Since this is not the case, τ instead serves as an approximation for the time at which the approximation (63) stops working. In fact, the approximation stops working a small amount of time before τ. This is expected since (61) does not make sense for $E > \sqrt{\epsilon^2 - \frac{\gamma^2}{4}}$ due to the domain of the arcsin.

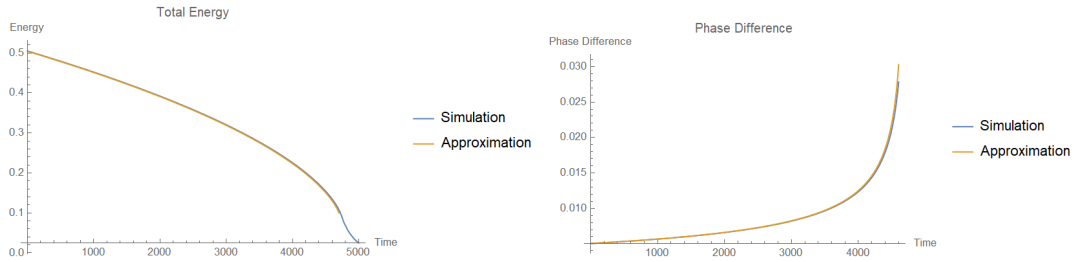

Figure 6: Graphs of the total energy and the phase difference for $E_0 = 0.505, \epsilon = -0.1, \gamma = 0.005$. (a) Is the total energy graphed from $t = 0$ to $t = \tau + 300 \approx 5000$ and (b) is the phase difference graphed from $t = 0$ to $\tau - 100 \approx 4600$.

Figure 6 shows the effectiveness of the approximation. E_0 was chosen so that it coincided with the initial energy of the graphs in the previous sections, leading to $\tau = 4700.8$. The energy was graphed for longer than τ to identify the behaviour after it leaves the breather, while the phase difference was graphed for less than τ since the expression for the approximation explodes due to the singularity in the arcsin. After this, we see that the behavior of the solution is governed either by (59) or (60). Note that by approximating the energy of the solution by the expression for the energy of the breather in (62) we are assuming that this approximation moves along the family of breathers and from Figure 6 we again see that this scenario accurately reproduces the observed numerical behavior of the solution of the system.

4.2 Metastable evolution of the three-site system

The method outlined in 4.1 for calculating the approximate time evolution of the metastable solution is unsuitable for systems with three or more sites. This is because the calculation would be too complicated or even impossible since it requires the analytical solution to the undamped breather in terms of the total energy. Nonetheless, a comparison between Figure 1 with Figure 2 shows they behave similarly. They both start with a very slow decay in the energy as the system drifts along a family of damped and driven breathers, with the drift being much slower in the three-site case. Eventually it reaches a point at which all the oscillators have the same energy. Shortly before reaching that point, the energy decay accelerates, with the effect on the three-site system being significantly more dramatic.

Moreover, we can numerically compute the bifurcations for the three-site undamped system in terms of E. For example, if $\epsilon < 0$, we find three bifurcations occurring at $E \sim 4.92|\epsilon|, E \sim 1.97|\epsilon|, E \sim 0.75|\epsilon|$. The undamped breather close to the metastable state ceases to exist for $E < 0.75|\epsilon|$. When the energies of the three sites are approximately all the same for the first time (at $t \sim 293\,800$ by looking at the numerical results), the total energy of the system is $\sim 0.063 = 0.63|\epsilon|$. The value

of the energy when it reaches this state is close to that of the bifurcation value for the undamped breather, just as in the two-site system.

Thus, we conjecture that the general evolution of these metastable states is as follows. When the trajectory is "captured" by one of the damped and driven breathers, the system begins to evolve by drifting along this family until the family of breathers disappears through bifurcation, at which point the system may be captured by another attractive family of approximately periodic orbits. There may, of course be other, possibly large, parts of the phase space where these metastable solutions do not exist and the evolution of the system is chaotic. In particular, it is not clear what properties of the periodic orbit in the undamped Hamiltonian system result in the solution becoming attractive once the system is subjected to damping.

5 Summary and Conclusions

In this paper we have derived a new family of periodic solutions of the damped and driven discrete nonlinear Schrödinger equation. We have derived approximations to these solutions and analyzed their stability. We have also proposed an explanation for the appearance of very long-lived metastable states in the phase space of weakly damped lattice systems in which the trajectory is attracted to a cylinder of such breathers and then drifts very slowly along the cylinder of breathers until this family of solutions disappears. We suspect that the disappearance occurs near a bifurcation of the undamped system. Finally, we have shown that certain aspects of the metastable states are better approximated by these damped and driven breathers than by the breather solutions of the undamped lattice system.

Acknowledgements: The research of CEW was supported in part by NSF grant DMS-18133. CEW also acknowledges many helpful conversations about breather solutions in the dNLS equation with J.-P. Eckmann. DAC is thankful for the support from Boston University's Undergraduate Research Opportunities Program.

References

[1] Stefano Iubini, Stefano Lepri, Roberto Livi, Antonio Politi, and Paolo Politi. *Nonequilibrium Phenomena in Nonlinear Lattices: From Slow Relaxation to Anomalous Transport*, pages 185–203. Springer International Publishing, Cham, 2020.

[2] C. Danieli, D. K. Campbell, and S. Flach. Intermittent many-body dynamics at equilibrium. *Phys. Rev. E*, 95:060202, Jun 2017.

[3] Carlo Danieli, Thudiyangal Mithun, Yagmur Kati, David K. Campbell, and Sergej Flach. Dynamical glass in weakly nonintegrable Klein-Gordon chains. *Phys. Rev. E*, 100:032217, Sep 2019.

[4] Martin Hairer and Jonathan C. Mattingly. Slow energy dissipation in anharmonic oscillator chains. *Communications on Pure and Applied Mathematics*, 62(8):999–1032, 2009.

[5] J.-P. Eckmann and C.E. Wayne. Breathers as metastable states for the discrete NLS equation. *Discrete & Continuous Dynamical Systems - A*, 38:6091–6103, 2018.

[6] Sergej Flach and Andrey V. Gorbach. Discrete breathers — advances in theory and applications. *Physics Reports*, 467(1):1 – 116, 2008.

[7] J.-P. Eckmann and C.E. Wayne. Decay of hamiltonian breathers under dissiptation. *Comm. Math. Phys.*, 380:71–102, 2020.

[8] Panayotis Panayotaros and Felipe Rivero. Multi-peak breather stability in a dissipative discrete nonlinear schrödinger (nls) equation. *Journal of Nonlinear Optical Physics & Materials*, 23(04):1450044, 2014.

[9] R S MacKay and S Aubry. Proof of existence of breathers for time-reversible or hamiltonian networks of weakly coupled oscillators. *Nonlinearity*, 7(6):1623–1643, nov 1994.

[10] S. Flach and C. R. Willis. Discrete breathers. *Phys. Rep.*, 295(5):181–264, 1998.

[11] P. G. Kevrekidis, K. Ø. Rasmussen, and A. R. Bishop. The discrete nonlinear Schrödinger equation: A survey of recent results. *International Journal of Modern Physics B*, 15(21):2833–2900, 2001.

[12] Noé Cuneo, Jean-Pierre Eckmann, and C Eugene Wayne. Energy dissipation in hamiltonian chains of rotators. *Nonlinearity*, 30(11):R81–R117, oct 2017.

[13] J.C. Eilbeck, P.S. Lomdahl, and A.C. Scott. The discrete self-trapping equation. *Physica D: Nonlinear Phenomena*, 16(3):318 – 338, 1985.

[14] Anne Greenbaum, Ren-Cang Li, and Michael L. Overton. First-order perturbation theory for eigenvalues and eigenvectors. *SIAM Review*, 62(2):463–482, 2020.